The American Association of Petroleum Geologists Bulletin
V. 67, No. 1 (January 1983), P. 166-177, 12 Figs.

Shallow Temperatures and Thermal Regime in the Hydrocarbon Province of Tierra del Fuego[1]

GARY W. ZIELINSKI[2] and PETER M. BRUCHHAUSEN[3]

ABSTRACT

A suite of shallow (<2 m deep) thermal measurements across the San Sebastian oil and gas field, northeastern Tierra del Fuego, indicates at least a 200 mWm^{-2} (5 HFU) thermal anomaly over the field. The anomaly appears to be of subsurface origin and, due to its magnitude, must be caused by a localized discharge of deep groundwater. A single published heat flow value and deep bottom hole temperature data for the area suggest a regional heat flow that is at least 20 mWm^{-2} (0.5 HFU) higher than the world average for similar tectonic provinces (post-Precambrian non-orogenic).

Maturation level estimates based on the heat flow and burial history of sediments suggest considerable lateral migration (at least 100 km) of hydrocarbons from deeper in the Magellan basin. From estimates of the timing of possible oil generation, minimum average migration velocity is within 1 or 2 orders of magnitude of the groundwater velocity required to cause the local and regional heat flow anomalies. This suggests that groundwater moving from deeper in the Magellan basin might simultaneously transport hydrocarbons and heat to the area. Volume flux estimates require that hydrocarbon concentrations significantly greater than possible via aqueous molecular solution.

INTRODUCTION

For more than a century, the association of hydrocarbon accumulations with thermal anomalies and groundwater flow has been frequently observed (Roberts, 1979). The cumulative weight of the observations has lead to several general theories on the role of moving groundwater in mobilizing hydrocarbons and in influencing their subsequent migration and accumulation (Hubbert, 1953; Meinhold, 1968, 1971; Roberts, 1979; Toth, 1980; Fowler, 1980). Recent reports on the distribution of heat flow over large hydrocarbon-producing sedimentary basins of central and western Canada reveal a correlation between the heat flow values and the large-scale hydrodynamics of the basins (Majorowicz and Jessop, 1981a,b). Particularly intriguing are reports from the Soviet Union of temperature anomalies present at a depth of only 1.2 m over individual hydrocarbon-producing structures (Artemenko and Malovitskiy, 1977; Osadchiy et al, 1978). If discernable temperature anomalies as high as a few degrees above background exist at shallow depth and are of deep origin, then tenfold heat-flow increases are implied. Such increases are consistent with convective vertical groundwater velocities on the order of 1 cm/yr, as implied by the heat flow observations of Majorowicz and Jessop (1981a,b). Furthermore, the results suggest that temperature effects of variations in surface boundary conditions such as diurnal and annual temperature oscillations, lateral changes in thermal properties, vegetation, insolation, and evaporation (Kappelmeyer and Haenel, 1974; Hillel, 1980) may be small in comparison with the inferred changes in heat flux from depth. Such variations in surface conditions have for conventional purposes restricted shallow-probe heat flow determination largely to the deep oceans.

In order to further investigate the relationship between geothermics, hydrology, and hydrocarbon accumulations and to test the usefulness of shallow thermal measurements in such investigations, a joint project was undertaken by researchers from Argentina's national oil company, Yacimientos Petroliferos Fiscales (YPF), the Lamont-Doherty Geological Observatory of Columbia University, and the Gulf Oil Corporation Research Center. As part of that project, from February 24 to March 4, 1980, a small expedition to the hydrocarbon province of northeastern Tierra del Fuego, Argentina (see inset, Fig. 1, hatched area) produced a small suite of shallow (<2 m deep) thermal measurements.

Tierra del Fuego was selected for this study because of a number of environmental factors and the presence of discrete oil and gas fields having well-defined limits of production. Deep bottom hole temperature measurements would be available to compare with shallow determinations. The environmental factors that we felt would increase chances of success would minimize variations in the surface boundary conditions that tend to dictate the shallow thermal regime. Much of eastern Tierra del Fuego, for example, is grassland with no significant change in surface vegetation and, hence, albedo. Topographic slopes are generally low enough to allow uniform ground exposure to insolation. The area is, furthermore, notorious for a high degree of annual cloud cover and persistently high winds. These tend to inhibit radiative ground heating in excess of ambient air tempera-

[1]Manuscript received October 29, 1981; accepted, May 14, 1982. Material in this paper was presented at the AAPG Research Conference, Temperature Environment of Oil and Gas, Santa Fe, New Mexico, September 13-17, 1981.

[2]Department of Geochemistry and Minerals, Gulf Science & Technology Company, Box 2038, Pittsburgh, Pennsylvania 15230.

[3]Lamont-Doherty Geological Observatory of Columbia University, Palisades, New York 10964.

We are indebted to E. C. Mainardi of Yacimientos Petroliferos Fiscales and his staff for the tremendous support provided throughout this project. The information and guidance of H. J. DiBenedetto proved extremely helpful. We gratefully acknowledge the field support provided by R. Barnes, R. Pombo, and A. Castro. Critical reviews by C. G. Kendall, I. Lerche, D. J. Toth, Y. P. Chia, and, particularly, thorough reviews by D. W. Baker and W. Roberts III led to improvements in the original manuscript. G. W. Hall provided valuable assistance with early logistics. Special thanks to T. J. Weismann for his confidence and support.

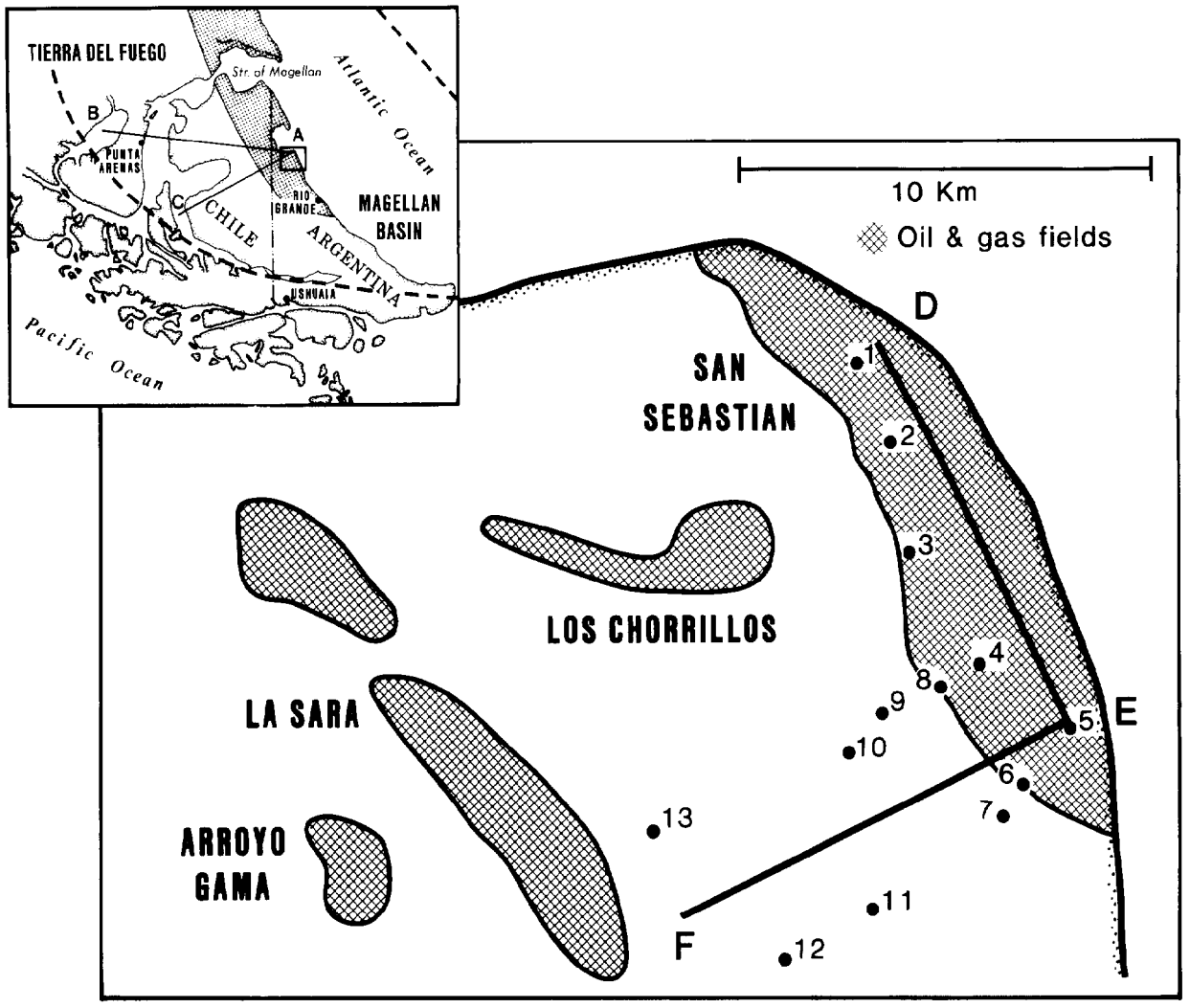

FIG. 1—Study area and location of thermal stations (numbered points). Hatched areas indicate location of hydrocarbon producing fields and (on inset map) Tierra del Fuego hydrocarbon province within the Magellan basin (dashed curves indicate approximate limits). AB and AC are sections in Fig. 10; lines DE and EF indicate trends used for projection of station data.

tures and to keep the air above the ground surface well mixed and, therefore, at a more uniform temperature. All of these factors together minimize lateral variations in surface temperature and cause ground temperatures, when averaged over a year, to be closer to the mean annual air temperature obtainable from weather data.

One other consideration in selecting the survey area was knowledge of peat deposits overlying parts of Tierra del Fuego and verified for our study area by YPF geologists. Because of easy penetration and the relatively low thermal diffusivity of peat, these deposits are a convenient medium for taking shallow heat flow measurements (Redfield, 1965a,b).

GEOLOGIC FRAMEWORK

The San Sebastian oil and gas field of Argentina lies within the hydrocarbon-producing province of the Magellan basin, northeastern Tierra del Fuego (inset, Fig. 1, hatched area). As is true of most of the province (Olea and Davis, 1977; Urien and Zambrano, 1977), production occurs within sandstones of the lower Cretaceous Springhill Formation (approximately 100 m thick) which overlies the Jurassic Tobifera Formation, a silicic volcanic sequence of ignimbrites, breccias, and tuffs (see Fig. 10). The Springhill Formation is overlain by a sequence of predominately claystones and siltstones grading to shales at depth. Total thickness of post-Jurassic sediments in the region is about 2,000 m. Individual hydrocarbon accumulations are largely controlled by topographic highs in the Tobifera Formation, against which the braided shoestring bodies of the Springhill Formation thin. This paleotopographic control is illustrated for the San Sebastian and La Sara fields on the regional seismic line (Fig. 2), which crosses both fields in a northeast-southwest direction parallel to line EF (Fig. 1). Reflectors terminate against the flanks of positive basement highs (highlighted), which also coincide with two major positive units or highs (arrows) indicated on structural maps of the area (Urien and Zambrano, 1977).

In the present study, the generalized post-Jurassic evolution of the Magellan basin (outlined by dashes, Fig. 1 inset) is especially important and is described in detail by Katz (1964), Zambrano and Urien (1970), Dalziel (1974), Olea and

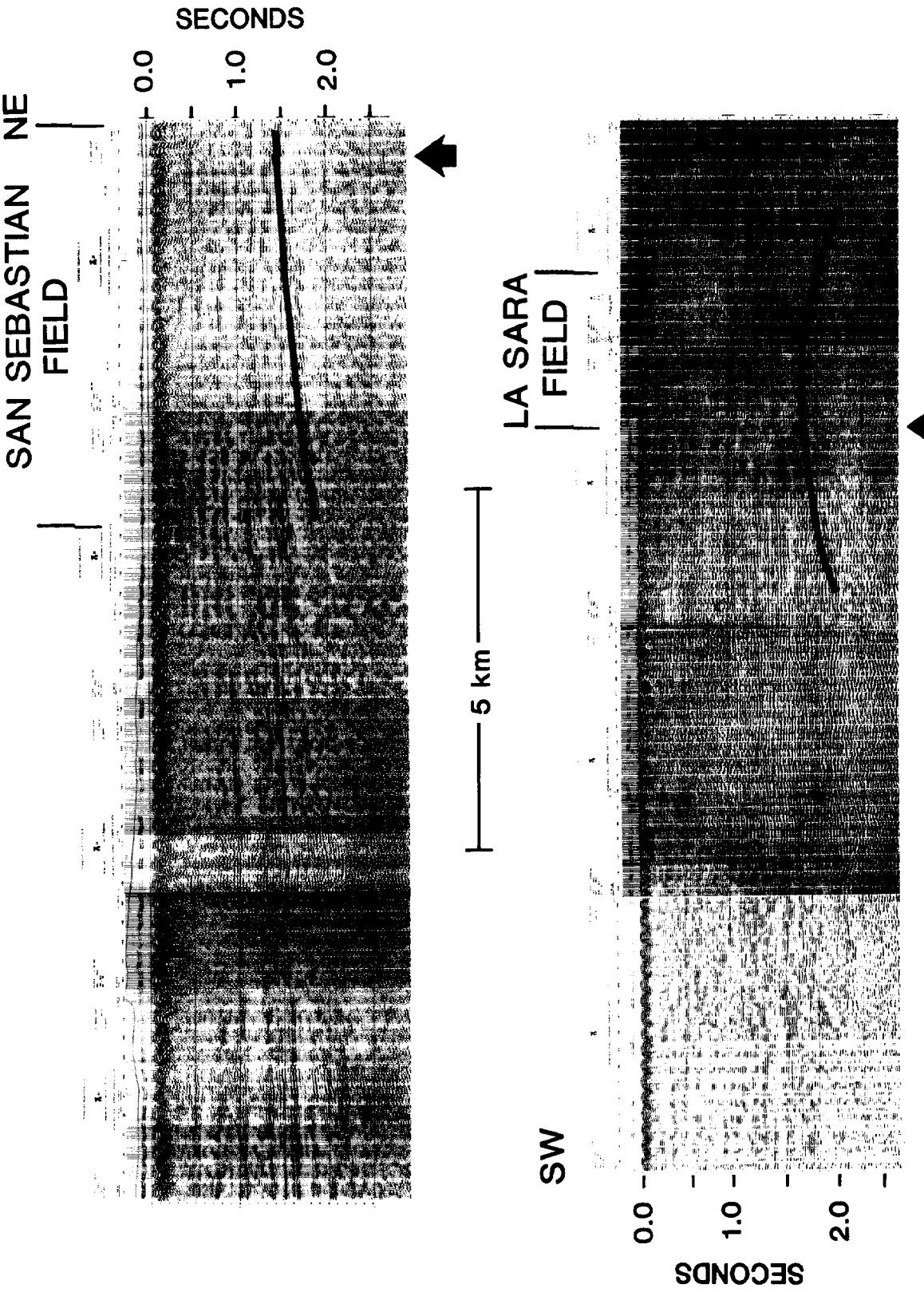

FIG. 2—Northeast-southwest trending seismic line crossing San Sebastian and La Sara fields. Arrows indicate major anticlinal structures.

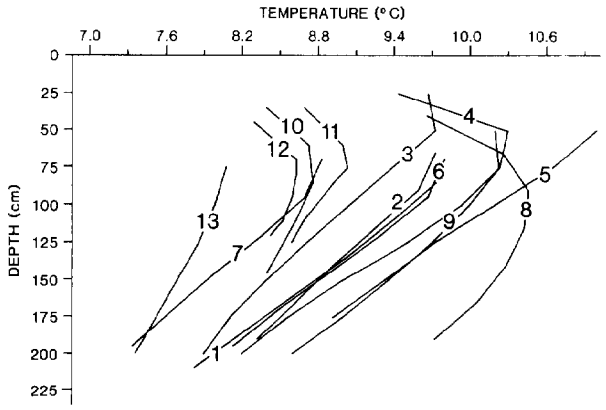

FIG. 3—Ground temperature profiles measured at each thermal station in Fig. 1.

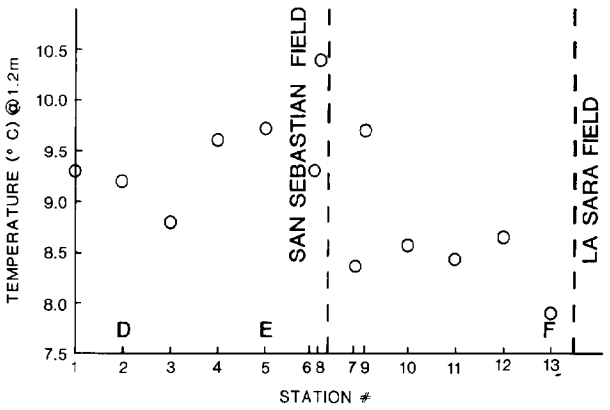

FIG. 4—Ground temperature at 1.2-m depth for each thermal station projected on lines DE and EF (Fig. 1). Vertical dashed lines indicate the relative location of the southwest boundary of the San Sebastian field and the northeast boundary of the La Sara field.

Davis (1977), Urien and Zambrano (1977), Bruhn and Dalziel (1977), Bruhn (1979), and others, The region from the eastern coast of Tierra del Fuego to the Andean Cordillera has largely been an area of geosynclinal sedimentation and subsidence, initiated during the Late Jurassic-Early Cretaceous. This followed a period of intense volcanism and extension probably associated with the penecontemporaneous opening of the South Atlantic (Rabinowitz and La Brecque, 1979) and the formation of a marginal basin to the west (Bruhn and Dalziel, 1977). Cenozoic subsidence was interrupted intermittently during phases of Andean orogeny. Most of the tectonic movement, however, took place in the Andean Cordillera and the westernmost part of the Magellan basin, whereas the eastern part encompassing the hydrocarbon province generally is regarded as stable platform.

TEMPERATURE MEASUREMENTS

Locations of thermal stations are shown in Fig. 1. Sites were prepared by hand-augering a number of 2-m deep holes, inserting 2 m by 1.3 cm (outer diameter) stainless steel tubing, and carefully filling the annulus with soil from the hole. The next day, sites were reoccupied and the temperature profiles inside the tubing measured by lowering a thermistor in 25-cm increments. The thermistor is a Fenwal Unicurve with a nominal resistance of 1000 Ω at 25°C, calibrated against a platinum resistance thermometer over a temperature range of 0° to 15°C. When temperature-resistance data are fit to a curve of the form $T^{-1} = A + B \log R + C (\log R)^3$ (Steinhart and Hart, 1968), where T is temperature (K), R is resistance (Ω), and A, B, and C are constants, a mean absolute value residual of 0.0006°C resulted. The thermistor output was monitored by a 4½ digit 30,000-count Keithley digital multimeter in the four-wire resistance mode and with <100 μA test current applied to the thermistor. Total relative instrument error is <0.002°C, with an absolute accuracy of about 0.02°C. In-situ repeatability based on measurements made on return trips of the thermistor is <0.01°C.

The 13 stations shown in Fig. 1 were completed within a 6-day period of time. The measured temperatures versus depth for each station are shown in Fig. 3. It was not possible to obtain measurements to the full 2-m depth at sites 10, 11, and 12 due to the presence of a gravel layer that could not be penetrated by the hand auger. Elsewhere the hand drilling was easily accomplished because of the soft consistency of the organic rich soils. The peat deposits in northeastern Tierra del Fuego are seasonally dry, as are those normally associated with steppe-type environments. This necessitated using the auger for penetration, although at some sites, tubing could be partly inserted without drilling. From Fig. 3, the most striking observation is that the range of temperatures measured at any given depth for all the stations is quite large, nearly 3°C. In addition, the lower-temperature stations occur preferentially off the San Sebastian field. Higher temperatures were measured over the field. This is also shown in Fig. 4, which is a plot of temperature at 1.2 m depth for each station with respect to the southwest boundary of the San Sebastian field. (Stations 1 through 5 trend parallel to the field and along line DE, while stations 6 through 13 are projected onto line EF, perpendicular to the field.) That boundary sharply marks the southwestern limit of production which is well defined by deep drilling. On the average, temperatures at 1.2-m depth appear to be about 0.5° to 1.0°C higher over the San Sebastian field (Fig. 4). This is of the same magnitude as the temperature anomalies reported at a similar depth over oil and gas fields in eastern Europe (Artemenko and Malovitskiy, 1977; Osadchiy et al, 1978). These anomalies, also associated with anticlinal producing structures, are attributed to ascending water.

RELATIVE HEAT FLOW

As discussed earlier, our survey area (Fig. 1) was chosen partly on the basis of the minimum likelihood of site-to-site differences in surface conditions, so that any significant temperature anomaly can then be related to a subsurface thermal condition. Still, having some quantitative means of verifying this assumption is desirable. One possible approach is to make use of the "indirect method" (Lee, 1977) to simultaneously obtain values of geothermal gradient and thermal diffusivity for individual site from corresponding temperature profiles. If site-to-site differences in the thermal diffusivity of the soils are assumed to be largely the result of

differences in thermal conductivity (that is, the product of the soil's density and its heat capacity remains relatively constant), then site-to-site changes in the product of the geothermal gradient and thermal diffusivity reflect relative differences in heat flow (heat flow equals the thermal conductivity multiplied by the gradient). A corresponding anomaly in the product of gradient and diffusivity would then imply additional heat input from depth.

The indirect method (Lee, 1977) relies on the fact that in the depth range of about 1 to 13 m, the major variation in ground temperature is due to an annual sinusoidal change in temperature at the surface. The resulting ground temperature distribution can be approximated mathematically by the equation:

$$T = T_S + gz + Ae^{-z\sqrt{\omega/2\mu}} \sin\left[\omega(t-t_0)-z\sqrt{\omega/2\mu}\right] \quad (1)$$

where T_S is the mean annual ground surface temperature, g is the geothermal gradient, A is the amplitude of the annual surface variation, and ω its angular velocity, t_0 is the time when $T=T_S$ at the surface, μ is the termal diffusivity of the ground (all are assumed constant), z is depth, and t is time. The applicability of this approximation to real ground conditions has been frequently demonstrated (e.g., Kelvin, 1861). Trigonometric expansion of equation (1) yields for any given depth z_i and time t_j:

$$T_{ji} = T_S + gz_i + \delta_j x_i + \epsilon_j y_i \quad (2)$$

where

$$\delta_j = A \sin \omega(t_j - t_0)$$

$$\epsilon_j = -A \cos \omega(t_j - t_0)$$

and

$$x_i = e^{-z_i\sqrt{\omega/2\mu}} \cos(z_i\sqrt{\omega/2\mu})$$

$$y_i = e^{-z_i\sqrt{\omega/2\mu}} \sin(z_i\sqrt{\omega/2\mu})$$

$$i = 1, 2, 3 \ldots m$$

Treating T_{ji} as the dependent variable and z_i, x_i and y_i as independent variables, equation (2) can be solved for $m \geq 5$ (that is, temperature values at five or more different depths are required) by least-squares fitting. Stepping through possible values of μ in discrete increments, a minimum root mean square (RMS) error in fit for a particular μ is taken to indicate the correct solution. That value of μ is interpreted as the weighted average thermal diffusivity for the depth range of the temperature measurements. The geothermal gradient, g, is obtained as a regression coefficient.

Due to the shallowness of the measurements, it was not possible to apply this procedure alone to the data from Tierra del Fuego. For typical soils, the annual temperature wave represented by equation (1) penetrates the ground with a wavelength λ given by

$$\lambda = \frac{2\pi}{(\omega/2\mu)^{1/2}}$$

which for a soil with a thermal diffusivity of 3×10^{-7} m^{2}sec^{-1} yields $\lambda = 11$ m. Thus only a small fraction of one wavelength of the annual wave is defined by our measurements. This proves insufficient for discrimination by the data reduction scheme, so additional constraints are required.

Figure 5 is a plot of the average daily air temperatures for a little over one year preceding our field work. Taken at Rio Grande airport, about 50 km south along the coast from San Sebastian, we feel they represent climatic and meteorologic conditions similar to those of our field area. As discussed earlier, because of the environmental conditions associated with this geographic area, the surface air temperature measurements might provide constraints on the ground surface temperatures, particularly when dealing with yearly averages. With this in mind a sinusoid is fitted to the data in Figure 5 to obtain estimates of the parameters $t-t_0$, T_s and A. These estimates are then used to constrain the temperature data reduction.

We first input (from Fig. 5) the value $t-t_0$ (~130 days) into equation (2) examined values of μg while stepping through a range of $\mu = 10^{-7}$ to 10^{-6} m^2 sec^{-1} by 10^{-8} m^2 sec^{-1} with $T_s = 5.63$°C and A varying independently. The procedure was then repeated, but with A = 5.60°C and T_s varying independently. We then progressively removed the shallower temperature measurements and observed the RMS error of the fit after each removal. In doing so, we found that comparatively large changes in the quality of the fit occurred for removal of points shallower than 120 cm for the data set as a whole. Removal of deeper points had considerably less effect. This is probably due to the presence of high-order harmonics in the shallower temperature data. Consequently, the temperature measurements at depths shallower than 120 cm were not used in the calculations by the Lee method. Because of insufficient penetration, reliable results could not be obtained by using the data from stations 10, 11, and 12. As a final check of the effectiveness of the data reduction scheme, the corrected temperatures (temperatures after the annual temperature wave was removed) were plotted with depth and screened for unacceptable curvature.

As a result of the procedure outlined above, 6 of the 13 stations yielded reliable results, as summarized in Figures 6 and 7. The circles in Figure 6 are values of ΔT_s, the difference between the mean annual temperature computed from the ground temperature data minus the $T_s = 5.63$°C

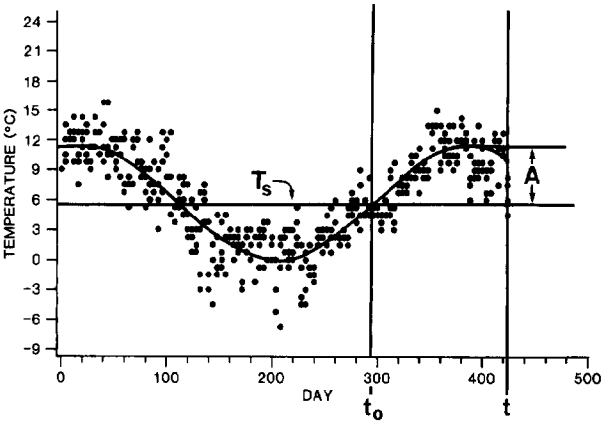

FIG. 5—Daily average surface air temperatures for Rio Grande for one year prior to field work. Solid line is best fit sinusoid. Mean annual temperature T_s, mean amplitude A of the variation, and time when $T = T_s$, t_0, are indicated by solid lines.

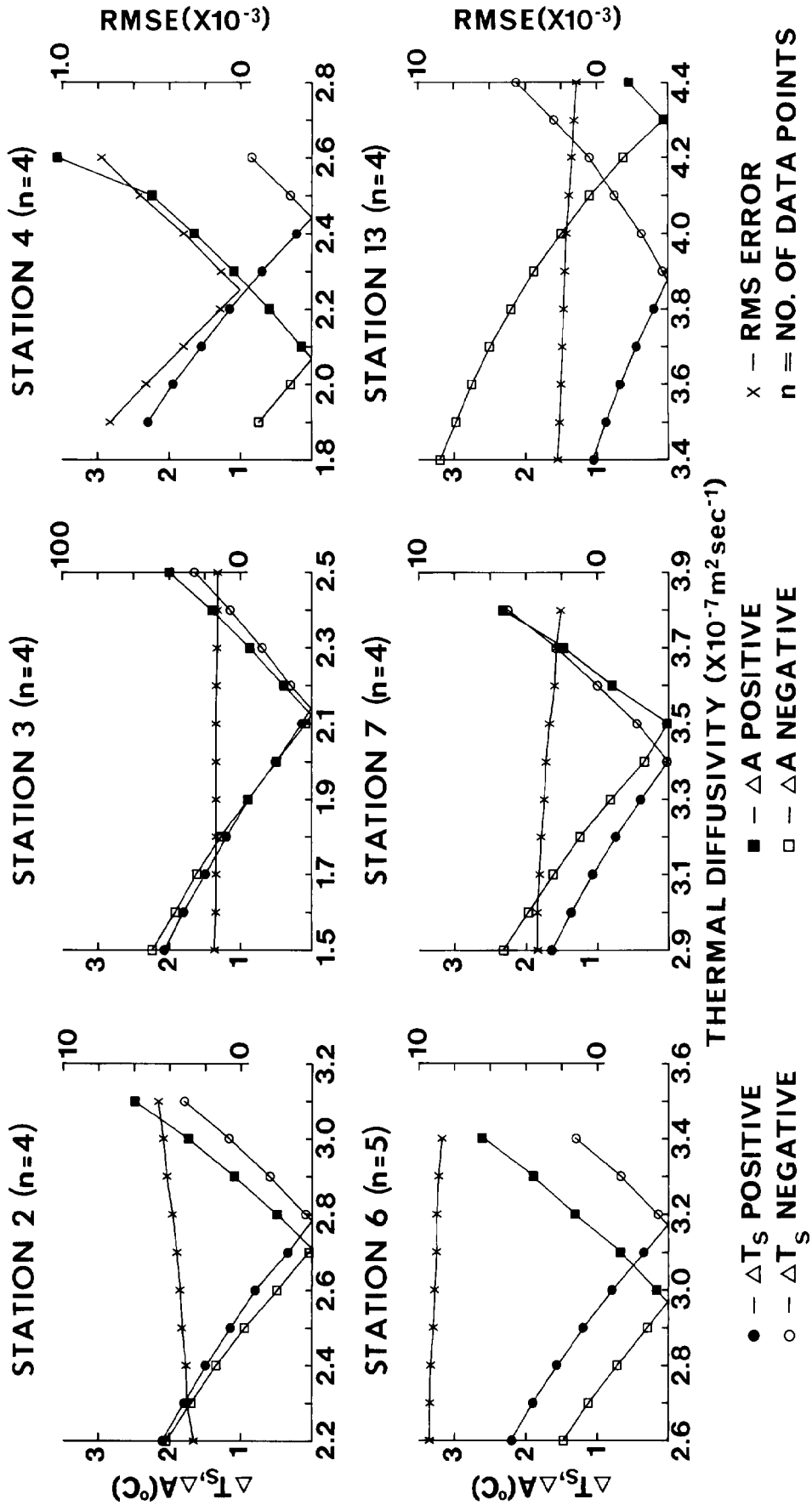

FIG. 6—Values of ΔT_s and ΔA, differences (ground-air) in mean annual temperature and amplitude, and RMS error of fit as a function of thermal diffusivity for each station that yielded a reliable value for μg, thermal diffusivity x temperature gradient. Points where circles and squares intersect indicate a combined best fit to weather data.

computed from the weather data (Fig. 5). Solid circles indicate positive values of ΔT_s, and open circles indicate negative values. These are plotted against the values of thermal diffusivity, μ, used for the particular regression. The squares in Figure 6 are, similarly, values of ΔA with respect to A = 5.60°C from the weather data. Plots for each of the successful stations are given in Figure 6 along with the RMS error for each regression as a function of μ. RMS errors are generally low and in the millidegree range. However, with the exception of station 4, there is little significant variation over the plotted range of parameters, so RMS error alone is not useful as a basis of selecting the correct solution. A minimum in RMS error does occur for station 4 for $\mu = 2.3 \times 10^{-7}$ m^2 sec^{-1} after specifying $t\text{-}t_0$ from the weather data. This particular regression is summarized in Figure 8. The solid circles are the measured temperatures, and the crosses are the linearized temperatures after removal of the annual wave. The solid curve shows the best-fit temperature profile from regression to the four deepest data points (RMS error equals 4×10^{-5} °C), and the dashed line is the best-fit background geothermal gradient. The best fit values of T_s and A computed from the ground temperatures measured at station 4 are shown in Figure 8 to be roughly within 1°C of the corresponding values implied by the weather data.

In Figure 6, $\Delta T_s = 0$ and $\Delta A = 0$ represent solutions in which the computed T_s and A equal the corresponding values computed from the air temperature data (Fig. 5). Where the lines connecting circles and squares intersect, a combined best fit to the weather station data is indicated. Station to station these intersections are fairly evenly distributed about the air temperature values, that is, they occur with both positive and negative values of ΔT_s and ΔA. For station 3, the intersection occurs extremely close to $\Delta T_s = \Delta A = 0$. All of the stations yield solutions within ±1°C of the air temperature parameters. Given the possible constraints imposed by the weather data, considerable uncertainty is still associated with choosing the correct value of μ. We are currently investigating methods of field measurements aimed at reducing this uncertainty. For this particular data set, however, the uncertainty in μg is always less than for μ or g individually. In order to assess the severity for our present purposes, we have plotted in Figure 7 the values of μg, normalized to values of T_s and A, as a function of station location (as in Fig. 4). Dashed lines denote positions of the San Sebastian and La Sara field boundaries. The horizontal line that runs through all three plots indicates the approximate value of μg based on deep production well measurements and arrived at as follows.

Uyeda et al (1978) published a single heat flow value of 96 mWm^{-2} (2.3 HFU, where 1 HFU = 1 μcal cm^{-2} sec^{-1}) for Tierra del Fuego about 50 km northwest of our survey area. This measurement is based on a gradient of 32 K km^{-1} obtained from bottom-hole temperature data and measured thermal conductivities averaging 3.0 Wm^{-1} K^{-1} (7.20 mcal cm^{-1} sec^{-1} K^{-1}). The average gradient based on 77 uncorrected bottom-hole temperature measurements from the San Sebastian and La Sara fields (provided by YPF) is 34.6 K km^{-1}, with a standard deviation of 2.5 K km^{-1}. This value is similar to the gradient reported by Uyeda et al (1978). Since the conductivities measured by Uyeda et al (1978) represent a lithology similar to that of our study area, one might interpret the similar gradients as implying similar heat flows. Rocks with thermal conductivities near 3 Wm^{-1} K^{-1} (7 mcal cm^{-1} sec^{-1} K^{-1}) characteristically have thermal diffusivities averaging about 14×10^{-7} m^2 sec^{-1} (Kappelmeyer and Haenel, 1974). Hence values of μg around 4 or 5×10^{-8} K m sec^{-1}

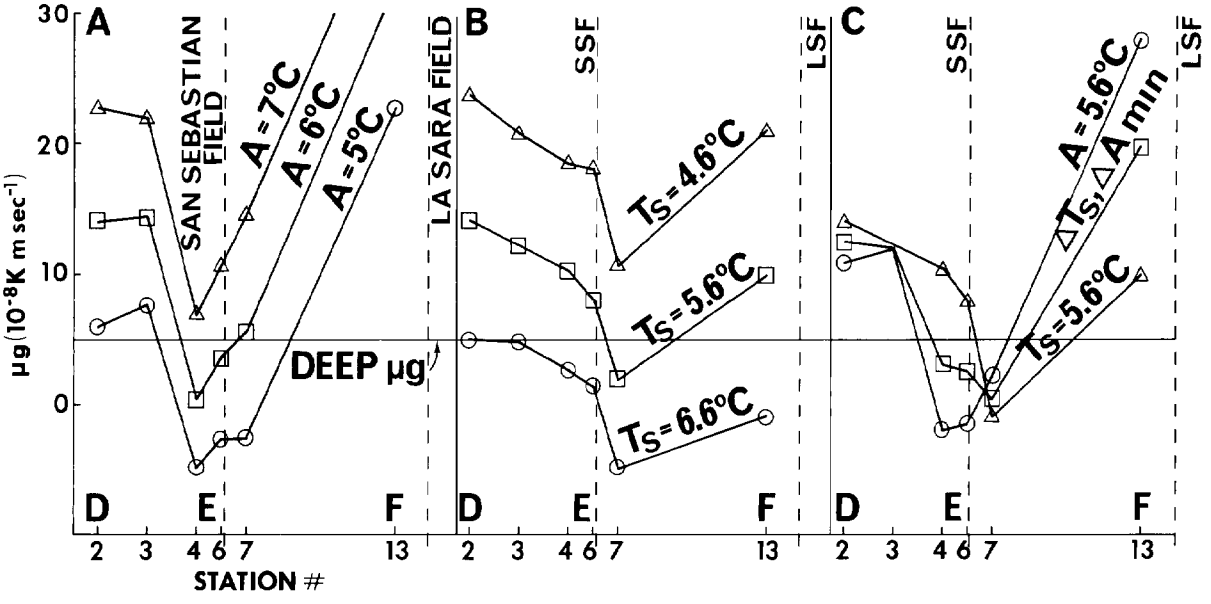

FIG. 7—Values of μg (thermal diffusivity versus temperature gradient) normalized to values of the amplitude A of the annual surface temperature variation (7a), mean annual surface temperature T_s (7b), and a combination of both (7c). T_s = 5.6°C and A = 5.6°C correspond to air temperature values from weather station observations (Fig. 5). Horizontal band indicates value of μg from deep production well data. Vertical dashed lines indicate relative positions of the San Sabastian and La Sara fields as in Fig. 4.

would be implied for the area by the deep well data. This estimate provides at least a rough absolute measure for evaluating our shallow determinations.

In Figure 7a the values of μg are plotted for A = 5 (circles), A = 6 (squares), and A = 7°C (triangles). The values between A = 5°C and 6°C would appear to be most evenly distributed about the deep μg. Recall that the air temperature value of A is 5.6°C. In Figure 7b, values of μg are plotted for T_s = 5.6°C, the mean annual ambient air temperature (squares), 1°C higher (circles), and 1°C lower (triangles). In this case, values of T_s corresponding with the weather station data also yield an average of μg in close agreement with the deep data. The range of values of μg from station to station is somewhat less in Figure 7b than in Figure 7a. This might imply slightly more random error associated with normalizing to constant A rather than to constant T_s. There is a bit of additional data to support this conjecture. Values of T s and A as products of the indirect method have been obtained at 18 sites in the offshore Salton Sea geothermal area (Lee and Cohen, 1979). If one first contours the values of T_s and then the values of A, similar values of T_s tend to cluster into groups. Isolated high and low values are spacially removed from the rest of the data. Doing the same for A yields a significantly more random spacial distribution. Therefore it may be that normalizing μg to constant values of T_s as in Figure 7b may be slightly more appropriate than normalizing to constant A (Fig. 7a). Ground temperature measurements made in areas of uniform vegetation reported by Kappelmeyer and Haenel (1974) suggest that over an area such as that encompassed by our stations (Fig. 1), the mean annual surface temperature should vary by no more than about 0.2°C.

We can visualize the net uncertainty in μg when constrained by both T_s and A computed from the meteorological data in Figure 7c. The triangles are values of μg for T_s = 5.6°C, and the circles are values of μg for A = 5.6°C. The squares are the values for combined closest agreement with the air temperature data and correspond to the intersections of constant T_s and A in Fig. 6. If we interpret the range of values for each station strictly as error limits, we are left with a significant difference in μg between stations 2 and 3 over the field and station 7 off the field. Stations 4 and 6 would at least be consistent with a systematic decrease in μg moving off the field. Station 13, most distant from the San Sebastian field and in closest proximity to the La Sara field, appears in Figure 7c to have a value of μg near or greater than the values obtained over the San Sebastian field. The results in Figure 7b, however, for T_s between 5.6°C and 6.6°C, indicate a value of μg for station 13 that is lower than μg for stations 2, 3, 4, and 6.

In Figure 9 the values of thermal diffusivity μ obtained from the data reduction are plotted for each station shown in Figure 7. The circles are for T_s = 5.6°C, and the squares are for A = 5.6°C. The values of μ obtained are well within the range acceptable for soils of varying degrees of moisture and organic content (Kappelmeyer and Haenel, 1974; Hillel, 1980). The station-to-station changes in μ (Fig. 9) are considerably greater than the differences between values obtained by alternately specifying T_s or A. Therefore, based on the thermal diffusivity measurements, no greater preference can be assigned to either normalization; however, as for the values of μg in Figure 7, there is slightly more variation in μ when normalizing to A than when normalizing to T_s. It should be noted, however, that the overall lateral variation in μ (a factor of 2) is considerably less than the lateral variation in μg (a factor of 10).

We feel that the overall results of our application of the Lee (1977) indirect method as summarized in Figure 7 tend to support the existence of a thermal anomaly associated with the San Sebastian field — the temperature anomaly seen at 1.2-m depth (Fig. 4) is predominately not due to local changes in thermal properties or surface boundary conditions and therefore must be of deeper origin. The magnitude of the anomaly in μg appears to be at least 5×10^{-8} K m sec $^{-1}$, which (if there is no great systematic change in the value of the density times the heat capacity of the soils) translates to a heat flow anomaly of at least 200 mWm $^{-2}$ (5 HFU).

In view of the magnitude of this anomaly, convective heat transport appears the only geologically plausible explanation. The lateral variation in implied heat flow (Fig. 7) seems, in general, to correlate with the lateral change in depth to Jurassic basement (Fig. 2). Most of the fields within the hydrocarbon province (where data are available) exhibit deep faulting associated predominately with the basement highs (Urien and Zambrano, 1977). This faulting could provide the avenues for vertical water migration, thus creating the surface heat flow distribution. If this is the case, the anomaly detected by shallow measurement would not be detectable using the deep well data (see Bredchoeft and Papadopulos, 1965), since gradients calculated from the latter are based on only two temperature points, one at the surface and one at near basement depth in the Springhill Formation.

DISCUSSION

The thermal anomaly implied by our measurements is of similar magnitude as those reported by Artemenko and

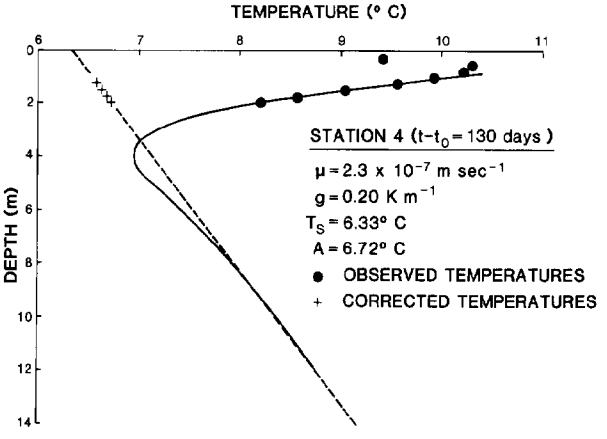

FIG. 8—Station 4 observed temperatures (closed circles) versus depth and temperature profile from regression (solid curve) to the four deepest temperature points assuming a sinusoidal annual surface temperature variation. Crosses are temperatures for the four deepest points with the annual temperature wave removed, and dashed line is the steady state geothermal gradient.

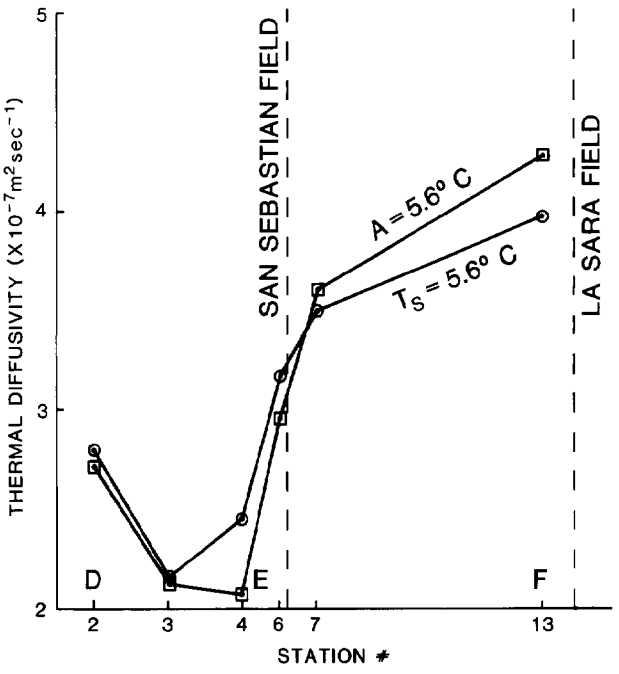

FIG. 9—Thermal diffusivity values obtained for each station normalized to A = 5.6°C (squares) and T_s = 5.6°C (open circles).

Malovitskiy (1977), Osadchiy et al (1978), and Majorowicz and Jessop (1981a, b). All are attributed to the transport of heat from depth by vertical water movement. The heat flow based on deep measurements in hydrocarbon-producing fields of northeastern Tierra del Fuego is about 96 mWm $^{-2}$ (2.3 HFU). This value is at least 20 mWm $^{-2}$ (0.5 HFU) higher than the world average for post-Precambrian non-orogenic areas (Lee and Uyeda, 1965), 64.4 mWm $^{-2}$ with a standard deviation of 15.9 mWm $^{-2}$ (1.54 HFU; standard deviation = 0.38). This average incidentally includes values from the interior lowlands of Australia, which are significantly higher than all other areas and may have been affected by Cenozoic volcanism (Lee and Uyeda, 1965). If one were to argue that the thermal anomaly detected by shallow measurement across the San Sebastian field was the result of ascending water, then there must be some source for the water being supplied to the region. Because basement is found at only 2-km depth within the hydrocarbon province, there is limited water available locally from compacting sediments. One possibility is that water is being supplied from deeper in the Magellan basin. If this water is required for localized upwelling (e.g., over San Sebastian field), it may also be capable of transporting the heat necessary to create the regional heat flow anomaly.

Figure 10 shows two generalized regional cross sections from the San Sebastian field to points representing maximum sediment accumulation in the Magellan basin. The sections were compiled from the isopach data of Zambrano and Urien (1970), Olea and Davis (1977), and Urien and Zambrano (1977). In order to obtain an estimate of the magnitude of the water flow velocity v required to create an additional 20 mWm $^{-2}$ (0.5 HFU) of heat flow in the oil province of Tierra del Fuego, we assume from Figure 10 a simplified geometry for the Magellan basin (Fig. 11), where X is the lateral distance from the oil province to deeper in the basin, L is the vertical distance to that deeper part of the basin, and v_z is the vertical component of the flow velocity. An estimate of v can be obtained from the following on-dimensional equation:

$$\frac{\partial^2 T}{\partial z^2} - \frac{\rho_w c_w v_z}{K}\frac{\partial T}{\partial z} = 0$$

$$T = T_0 \quad (z = 0)$$

$$T = T_L \quad (z = L)$$

where ρ_w and c_w are the density and heat capacity of water, and K is the thermal conductivity of the sediments. A solution for temperature T in terms of the temperatures at the surface, To, and at depth z = L, T_L is (Bredehoeft and Papadopulos, 1965):

$$\frac{T - T_0}{T_L - T_0} = \frac{e^{\frac{\beta z}{L}} - 1}{e^{\beta} - 1} \tag{3}$$

where

$$\beta = \frac{\rho_w c_w v_z L}{K}. \tag{4}$$

The corresponding surface heat flow is

$$-K\frac{\partial T}{\partial z}\Big|_{z=0} = -K\frac{T_L - T_0}{L}\frac{\beta}{e^{\beta} - 1}. \tag{5}$$

From equation (5) it can be seen that the effect of water flow is to alter heat flow by the factor

$$\frac{\beta}{e^{\beta} - 1} \tag{6}$$

If we assume for eastern Tierra del Fuego a maximum background heat flow of 80 mWm $^{-2}$ (1.9 HFU), which is the post-Precambrian, non-orogenic average plus 1 standard deviation, this would imply $\frac{\beta}{e^{\beta}-1} \cong 1.2$ to obtain a total heat flow as observed, 96 m Wm^{-2} (2.3 HFU). From Figure 10, we have L/X ≅ 1/30. If we assume $\rho_w c_w \cong$ 1 cal/cc K K = 3 Wm $^{-1}$ K $^{-1}$ (7 mcal cm $^{-1}$ sec $^{-1}$ K $^{-1}$), and L = 5 km, then we obtain from equations (4) and (6) the result that v ≅ -1.6 x 10 $^{-9}$ m sec $^{-1}$ (the negative sign denotes an upward vertical component), or about 5 cm yr $^{-1}$ is the water velocity necessary to cause the observed regional heat flow anomaly by convection. This is of the same order as that predicted by Majorowicz and Jessop (1981a, b) for Canadian sedimentary basins.

If we further assume that the water flow on a regional scale obeys Darcy's law, then

$$v = -K^*\frac{dh}{dx}$$

where K* is the hydraulic conductivity of the sediments and dh/dx is the horizontal gradient in head. The Springhill Formation probably represents optimum permeability conditions for lateral water movement in the Magellan basin. Measured at 1000 md (Urien and Zambrano, 1977), this translates into a

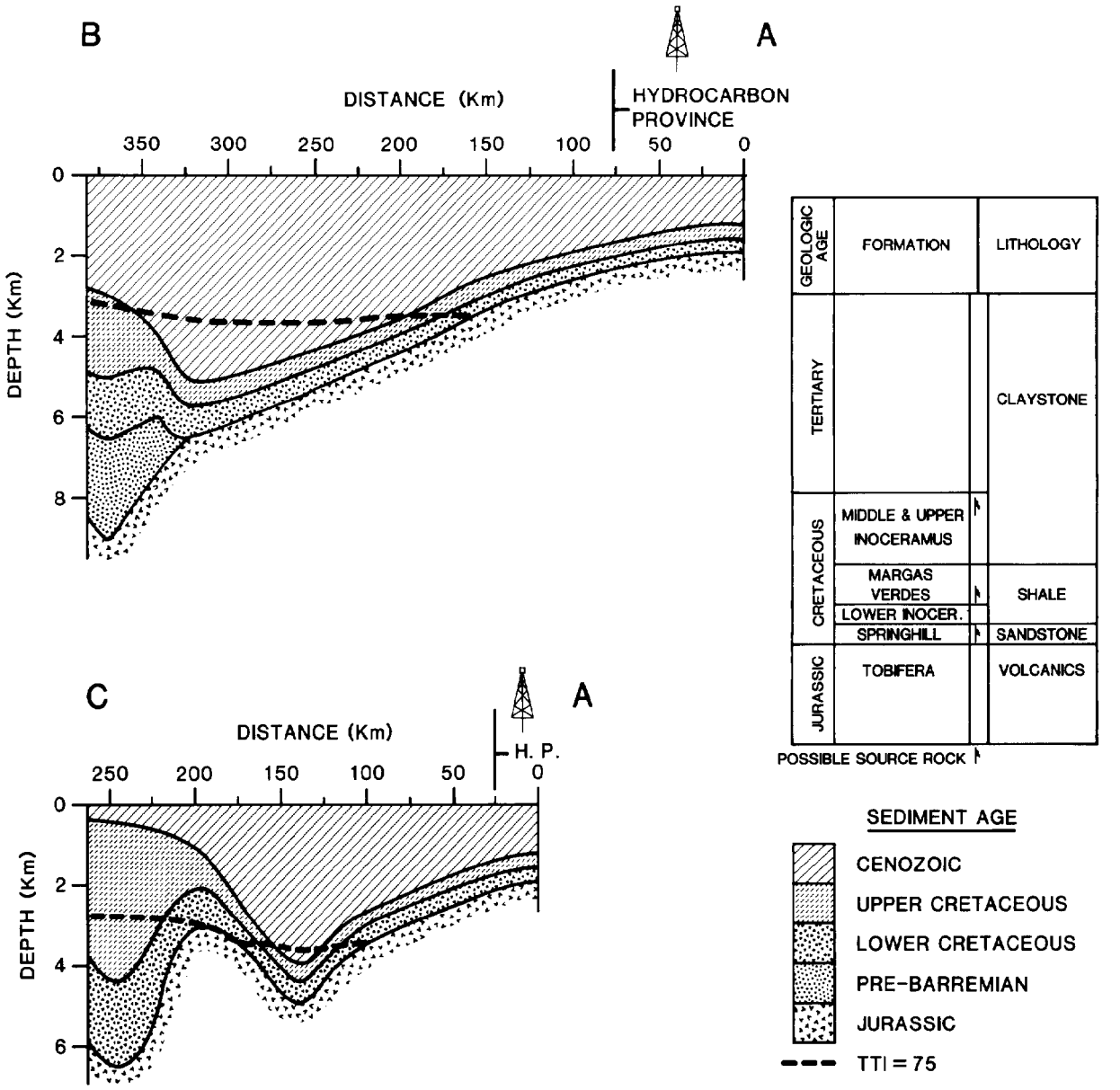

FIG. 10—Generalized lithologic and stratigraphic cross sections in Magellan basin (location in Fig. 1) compiled from published data. Dashed lines indicate TTI (time-temperature index) equal to 75. Flags indicate the stratigraphic location of possible source rocks.

hydraulic conductivity of about 10^{-5} m sec^{-1}. With this value for K* and v = 1.6 x 10^{-9} m sec^{-1}, then dh/dx would be at least 1.6 x 10^{-4} in order to satisfy Darcy's Law. According to Magara (1978), typical sedimentary basins have horizontal head gradients (due to excess pore pressure) from 1/20 to 1/200. This is 1 to 2 orders of magnitude greater than the dh/dx needed. In addition, in Tierra del Fuego there is about a 500-m difference in elevation between the oil province and the western edge of the Magellan basin where the deepest basinal units outcrop (e.g., Olea and Davis, 1972; Bruhn and Dalziel, 1977). This can give rise to a horizontal gradient in gravitational head of 10^{-3}, which itself is greater than that required to satisfy Darcy's Law in the Magellan basin. For such values of head gradient, Darcy's Law would be satisfied even for permeabilities corresponding to claystones (see Magara, 1978, Table 9-1), which comprise a significant part of the lithology of the Magellan basin (see Fig. 10). We admit that our application of Darcy's Law is an oversimplification; however it is significant that these calculations cannot preclude the large-scale groundwater flow necessary to create the regional heat flow anomaly in northeastern Tierra del Fuego.

We discussed earlier and showed some evidence for the implied relation between hydrocarbon accumulations and localized deep water discharge. We also suggested a connection between this localized vertical upwelling and large-scale lateral water movement in the Magellan basin. We now explore for possible links between the large-scale groundwa-

ter movement and basinwide hydrocarbon generation and migration. For this purpose, we use the Lopatin's (1971) time-temperature index (TTI), as calibrated by Waples (1980) and defined by the equation

$$TTI = \int_0^{t'} 2^{\frac{T(t)-105}{10}}\, dt$$

where T and t are temperature in °C and time in millions of years, respectively. This equation treats the maturation of organic matter as a kinetic process in which the reaction rate doubles with every 10°C rise in temperature. Using the stratigraphic data from Figure 10 for time-depth control and assuming as an upper limit a constant geothermal gradient of 40 K km^{-1}, we compute TTI for vertical columns of sediments at a number of locations along sections AB and AC. Details of this procedure are described by Waples (1980). No attempt is made to account for unconformities in the stratigraphic columns; however, in view of the general subsidence history of the eastern half of the Magellan basin, this should not constitute a serious omission. We then note the present-day depths at which TTI = 75 for each column (Fig. 10). This provides an estimate of the minimum depths in the Magellan basin at which sedimentary organic matter has reached sufficient thermal maturity to be in the main stage of oil generation. The underlying assumption is that the mechanism of oil generation in the Magellan basin is similar to that postulated for other world sedimentary basins. If this is the case, the interesting result is that none of the sediments overlying the Jurassic volcanics within the hydrocarbon province of Tierra del Fuego are likely to have generated oil. The nearest points in the basins where sediments reach a TTI = 75 occur at least 100 km to the west and south of the hydrocarbon province. This implies that in order for oil and gas to be present in the hydrocarbon province, secondary or tertiary migration over lateral distances of 100 km or more must have taken place. The geothermal gradient used for these calculations (40 K km^{-1}) reflects an upper limit to the regional heat flow, which is among the highest by world standards. It is not likely, therefore, to have been sufficiently higher in the past so as to significantly alter our TTI results. This gradient, which also exceeds published values for the Andean Cordillera (Uyeda et al, 1978), would have to be doubled in order to obtain a TTI = 75 within the hydrocarbon province.

For progressively deeper vertical columns in the Magellan basin, we also calculate the earliest time at which any sediment reached a TTI = 75, and plot this time against lateral distance from the hydrocarbon province (Fig. 12). The circles are for section AB and the crosses are for section AC. The slopes of the two straight lines that bound the data specify a range of minimum lateral migration velocity necessary for hydrocarbons to reach the hydrocarbon province from points deeper in the Magellan basin by the present day. The range of velocity (0.17 to 0.55 cm yr^{-1}) approaches to within 1 order of magnitude the minimum water flow velocity necessary to cause the regional heat flow anomaly observed in the hydrocarbon province. This result suggests a possible causal connection. The ratio of the hydrocarbon migration velocity to the water flow velocity implied by our estimates is 10^{-1} or 10^{-2}. If these velocities represent a volume flux of fluid (that is, a volume of fluid passing across a unit of area per unit time), then this ratio can be interpreted as an average concentration of hydrocarbons carried by the water (assuming the water is transporting the hydrocarbons). Although considerable uncertainty surrounds the estimate of this concentration, it is several orders of magnitude greater than that possible if transport occurred with the hydrocarbons in strictly aqueous solution (Price, 1976). The solution mechanism alone, therefore, seems unable to account for the large-scale hydrocarbon migration postulated for the Magellan basin. The similarity of regional migration velocities for both water and hydrocarbons may also be indicative of similar pathways of migration. Despite the degree of interdependence, the mode or modes of transport may be velocity-limited by the same permeability barriers.

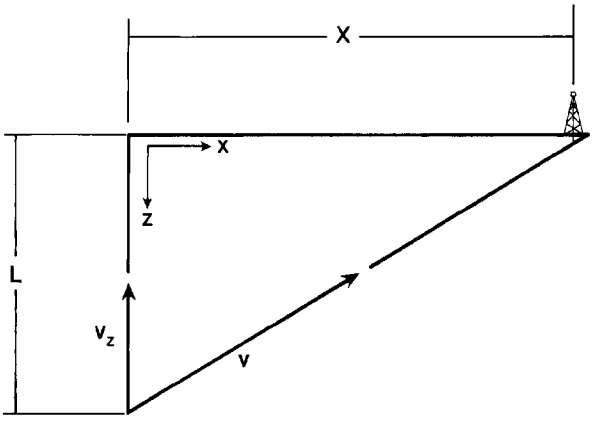

FIG. 11—Simplified geometry used for estimating groundwater flow velocity v in the Magellan basin from heat flow data. Well symbol indicates the hydrocarbon province.

If this regional water movement eventually results in local fault-controlled vertical discharge in the hydrocarbon province (as was suggested), equations (4) and (5) can be used to estimate the vertical flow rate of v_z implied by the 200 mWm^{-2} (5 HFU) San Sebastian heat flow anomaly. If the regional heat flow

$$-K\,\frac{T_L - T_0}{L} = 96\ \text{mWm}^{-2}\ (2.3\ \text{HFU})$$

we then require

$$\frac{\beta}{e^{\beta}-1} \cong 2 \quad \text{or} \quad \beta \cong 1.6$$

From equation (4), it is interesting to note that if the vertical flow originates somewhere in the lower fourth of the total 2,000 m of sediments in the San Sebastian area (that is, L = 1.5 km), then a value for v_z of -1.6×10^{9} m sec^{-1} (5 cm yr^{-1} is obtained. This flow rate is identical to the value obtained for the regional water movement in the Magellan basin.

CONCLUSIONS

We present data that support the presence of hydrocarbon-related thermal anomalies and their identifica-

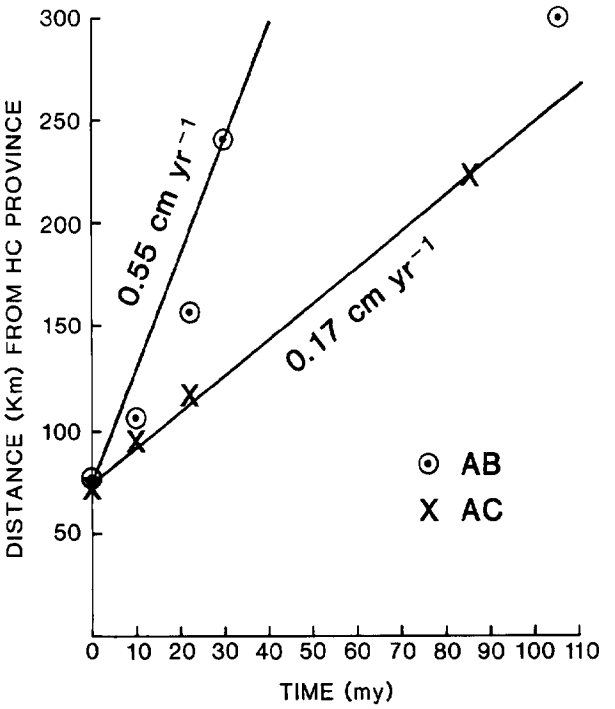

FIG. 12—Distance of lateral oil migration to the hydrocarbon province versus time of earliest oil generation (TTI = 75) for points deeper in the Magellan basin. Circles are for section AB, and crosses for section AC (Fig. 1). Slopes of lines which bound the data indicate velocities from 0.17 to 0.55 cm/yr.

tion by shallow temperature measurement. Transport of heat by moving groundwater is a viable cause for these local thermal anomalies as well as for the regional anomaly suggested for northeastern Tierra del Fuego. We interpret the latter as being due to regional water movement from deeper in the Magellan basin, and we further suggest that this same mechanism might also be related to the presence of hydrocarbons in northeastern Tierra del Fuego, since maturation studies do not support their generation locally.

REFERENCES CITED

Artemenko, V. I., and Y. P. Malovitskiy, 1977, Results of a bottom geothermal survey in the Bakhar oil-gas field: Petroleum Geology (USSR), v. 15, 1978, p. 150-152.

Bredehoeft, J. D., and I. S. Papadopulos, 1965, Rates of vertical groundwater movement estimated from the earth's thermal profile: Water Resources Research, v. 1, p. 325-328.

Bruhn, R. L., 1979, Rock structures formed during back-arc basin deformation in the Andes of Tierra del Fuego: Geol. Soc. America Bull., v. 90, p. 998-1012.

——— and I. W. D. Dalziel, 1977, Destruction of the Early Cretaceous marginal basin in the Andes of Tierra del Fuego, *in* M. Talwani and W. C. Pitman III, eds., Island arcs, deep sea trenches and back-arc basins: (Maurice Ewing Ser.) Wash., D.C., American Geophysical Union, v. 1, p. 395-405.

Dalziel, I. W. D., 1974, Evolution of the margins of the Scotia Sea, *in* C. A. Burk and C. L. Drake, eds., The geology of continental margins: New York, Springer-Verlag, p. 567-579.

Fowler, P. T., 1980, Telling live basins from dead ones by temperature: World Oil, May, p. 107-122.

Hillel, D., 1980, Fundamentals of soil physics: New York, Academic Press.

Hubbert, M. K., 1953, Entrapment of petroleum under hydrodynamic conditions: AAPG Bull., v. 37, p. 1954-2026.

Kappelmeyer, O., and R. Haenel, 1974, Geothermics with special reference to application: Geoexploration Monographs, Germany, Gebruder Borntraeger, Ser. 1, n. 4.

Katz, H. R., 1964, Some new concepts on geosynclinal development and mountain building at the southern end of South America, *in* Proceedings of the 22nd Internat. Geol. Cong. (New Delhi) v. 4, p. 241-255.

Kelvin, Lord, 1861, The reduction of observations of underground temperature, Royal Soc. Edinburgh Trans., v. 22, p. 405.

Lee, T.-C., 1977, On shallow-hole temperature measurements — a test study in the Salton Sea geothermal field: Geophysics, v. 42, p. 572-583.

——— and L. H. Cohen, 1979, Onshore and offshore measurements of temperature gradients in the Salton Sea geothermal area, California: Geophysics, v. 44, p. 206-215.

Lee, W. H. K., and S. Uyeda, 1965, Review of heat flow data, *in* W. H. K. Lee, ed., Terrestrial heat flow: Geophysical Monograph Ser., no. 8, p. 87-190.

Lopatin, N. V., 1971, Temperature and geologic time as factors in coalification (in Russian): Akad. Nauk SSSR Izv. Ser. Geol., no. 3, p. 95-106.

Magara, K., 1978, Compaction and fluid migration: New York, Elsevier, Developments in Petroleum Science, no. 9.

Majorowicz, J. A., and A. M. Jessop, 1981a, Regional heat flow patterns in the Western Canadian sedimentary basin: Tectonophysics, v. 74, p. 209-238.

——— and A. M. Jessop, 1981b, Present heat flow and a preliminary paleogeothermal history of the central Prairies basin, Canada: Geothermics, v. 10, p. 81-93.

Meinhold,R., 1968, Der Zusammenhang zwischen Geothermik, Hydrodynamik, Geochemie and Erdollagerstätten, Erdöl-Erdgas-Erkundung und Förderung; Leipzig, VEB Verlag, v. I, p. 422-433.

——— 1971, Hydrodynamic control of oil and gas accumulation as indicated by geothermal, geochemical and hydrological distribution patterns: Eighth World Petroleum Congress, v. 2, p. 55-56.

Olea, R. A., and J. C. David, 1977, Regionalized variables for evaluation of petroleum accumulation in Magellan basin, South America: AAPG Bull., v. 61, p. 558-572.

Osadchiy, V. G., et al, 1978, Geothermal and geochemical anomalies in the Svidnitsko-Kokhanov gas-oil field: Petroleum Geology (USSR), v. 15, 1978, p. 546-547.

Price, L. C., 1976, Aqueous solubility of petroleum as applied to its origin and primary migration: AAPG Bull., v. 60, p. 213-244.

Rabinowitz, P. D., and J. L. La Brecque, 1979, The Mesozoic South Atlantic Ocean and evolution of its continental margins: Jour. Geophys. Res., v. 84, p. 5973-6002.

Redfield, A. C., 1965a, The thermal regime in salt marsh peat at Barnstable, Massachusetts: Tellus, v. 17, p. 246-259.

——— 1965b, Terrestrial heat flow through salt-marsh peat: Science, v. 199, p. 1219-1220.

Roberts, W. H., III, 1979, Some uses of temperature data in petroleum exploration: paper presented at Symposium II, Unconventional Methods in Exploration for Petroleum and Natural Gas, Dallas, September 13-14.

Steinhart, J. S., and S. R. Hart, 1968, Calibration curves for thermistors: Deep-Sea Research, v. 15, p. 497-503.

Toth, J., 1980, A general hydraulic theory of petroleum migration, *in* W. H. Roberts, III, and R. J. Cordell, eds., Problems in petroleum migration: AAPG Studies in Geology 10, p. 121-167.

Urien, C. M., and J. J. Zambrano, 1977, Southern Argentina Magallanes and Malvinas basins, geologic exploration guide: Houston, Servicios Ryder Scott, S.A., v. 1.

Uyeda, S., et al, 1978, Report of heat flow measurements in Chile: Bull. Earthquake Res. Inst., v. 53, p. 131-163.

Waples, D.W., 1980, Time and temperature in petroleum exploration: AAPG Bull., v. 64, p. 916-926.

Zambrano, J. J., and C. M. Urien, 1970, Geological outline of the basins in Southern Argentina and their continuation off the Atlantic shore: Jour. Geophys. Res., v. 75, p. 1363-1396.